

Finite element analysis of a glass structure in a superyacht superstructure

Abstract

Recent tendencies in superyacht designs have been accompanied by the enlargement of the dimensions of yacht windows. Yacht designers are motivated by the requests of yacht owners to increase the transparency of their vessels to offer panoramic views of the surroundings while being shielded from the elements. Current standards for yacht windows consider window panes to be mechanically independent of the adjacent ship structure, limiting the size of uninterrupted glazed areas. In this study, a section of the top deck of a yacht fully enclosed by glass is investigated, with glass panels spanning from deck level to the top of the yacht. The edges of the glass panels are connected to transverse portal frames. The behaviour of the structure was assessed in response to loads set forth by classification societies for the design of yacht structures. These loads correspond to specific wave conditions a yacht is expected to sail in and include external pressures, inertial loads and gravity. A finite element model was created through which the mechanical behaviour of the structure was calculated. A parametric study is performed in which the behaviour of simplified beam-panel connections and different glass panel thicknesses are assessed. The use of a surface-to-surface contact function in Abaqus, which approximates the behaviour of adhesive bonding between the beams and the panels in the glass structure, is also demonstrated.

Keywords

Structural glass, Ship structure, Superyacht, Finite element analysis, Marine glazing

1. Introduction

Over the last decade, the size of glazed areas in superyachts have been gradually increasing. Superyacht designers are motivated to increase the size of windows in the vessel for the enjoyment of passengers and superyacht owners. By increasing the transparency of the ship, designers strive to give passengers spectacular views of the surrounding environment and to allow more natural light into the ship. Large glazed areas are also aesthetically appealing, giving it a unique appearance compared to other ships, which may add to the exclusivity superyacht owners seek (Gizzi & Bennison, 2009; Moupagitsoglou, 2020; Verbaas, 2012).

However, the dimensions of each window in ship structures are usually rather limited. Glazed areas are interrupted by structural components, such as steel or aluminium profiles, which are necessary for the structural integrity of the ship (Boote & Vergassola, 2016). Due to the high brittleness of glass and its varying breaking strength, shipbuilders have been reluctant to use glass as a load-bearing component (Jansen, 2014). Furthermore, the guidelines and technical standards of classification societies, according to which ships are typically built, do not prescribe regulations for the use of glass as an integral load-bearing component in a ship's structure. The ISO standard 'Large Yachts – Strength, weathertightness and watertightness of glazed openings' (ISO 11336-1 (2012), ISO 11336-2 (2020) and ISO 11336-3 (2019)) is often referenced by classification societies for the design of yacht windows where the mechanical behaviour of the glass pane is considered independent from that of the surrounding structure. Therefore, the single window panes are not expected to take on any loads from the surrounding yacht structure and they do not contribute to the overall stiffness of the ship (Wiegard et al., 2018). Instead, according to ISO 11336-1 (2012), the strength of the glass panes in yacht windows are to be determined for a design pressure

acting perpendicular to the glass surface. As an example, ISO 11336-1 (2012) presents Equation 1 for the calculation of the minimum thickness of a rectangular monolithic glass pane, where t is the minimum thickness of the pane, b_P is the short side of the rectangular pane, β is a coefficient for the pane aspect ratio, p_D is the design pressure and σ_A is the allowable design flexural stress of the glass.

$$t = b_P \sqrt{\frac{\beta p_D}{1000 \sigma_A}} \quad (1)$$

Preventing the deforming yacht structure from loading the glass pane is typically solved by using a flexible adhesive to bond the glass to a metal frame (ISO, 2020; Wiegard et al., 2018).

Permitting glass to take on the loads within a ship's structure, would present a solution to further increase the size of glazed areas as it would reduce the necessity for conventional structural materials. However, little is known about the behaviour of glass as a structural component in the structure of a ship. Major differences between land-based structures and ships have also prevented design standards for structural glass to be transferred from land to sea. As opposed to buildings, ships are constantly flexing due to hydrodynamic forces and accelerations caused by waves. In severe weather conditions, ships should also be able to withstand a combination of high wind loads and the impact of high waves. Ships can also be subject to a larger variety of weather conditions compared to those experienced by buildings, which may also be more extreme. This is due to the ability of a ship to travel through different climates (Wium et al., 2022).

The work presented in this paper is part of a larger investigation into the structural capabilities of glass in superyachts, or yacht structures. In this study, finite element analyses are performed on a novel glass structure concept in the superstructure of a yacht. The superstructure is the part of the ship structure above the main deck of the hull. Unlike the glass panes in conventional yacht windows, the glass in the structure is treated as an integral parts of the superstructure, exposed to all loads conventional structural components in this area of the ship are required to resist. The purpose of the study is to show how the strength of glass and the ways in which it is connected can be used to increase the reliance on the structural capabilities of glass and reduce the necessity of conventional metallic structures.

A parametric study is performed to assess the behaviour of the glass structure with regards to different yacht load cases. The behaviour of the glass structure is determined for three connection types between glass panels and steel portal frames. In addition, three glass panel thicknesses are compared.

2. Glass structural concept

Fig. 1 shows the glass structure concept, which is located on the top deck of the yacht. The glass structure is conceptualized using a 3D model of the yacht structure of an existing 90 m yacht. The glass structure is 12 m in length and covers the full 10 m width of the deck. Fig. 1a also shows the coordinate system, which was used in this study. The main dimensions of the glass structure are shown in Fig. 2. The location of the glass structure is chosen for its potential of offering significant transparency in an area of the superstructure where a large expanse of glazing would be most suitable for passengers. In the original design of the yacht, this area of the deck is used for leisure with a living room opening up to an open deck. Therefore, the area does not need to be subdivided by bulkheads for cabins or technical rooms. Being located in the top tier of the superstructure also allowed for the creation of a glass structure which fully encloses the deck, with glass panels acting as side walls and as a ceiling or roof. This differs significantly from previous yacht designs where windows typically only extend from the deck level to the ceiling.

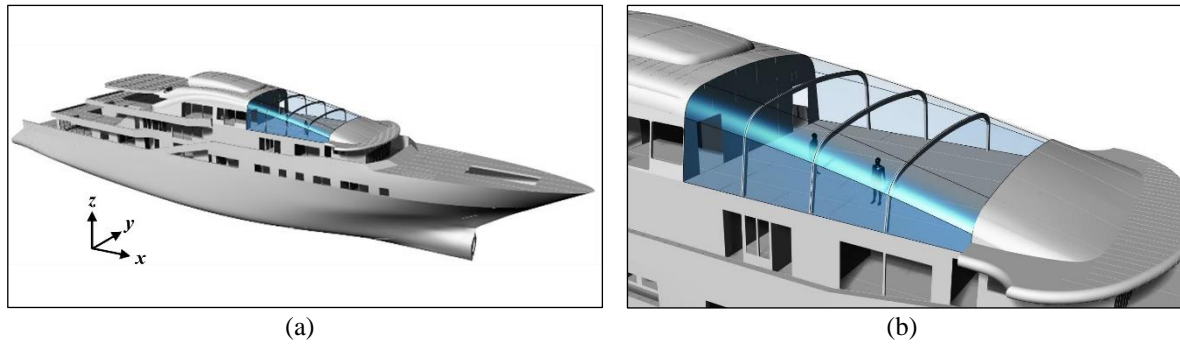


Fig. 1: a) Global view of yacht 3D model with glass structure. b) Detailed view of glass structure in superstructure.

The structure consists of large glass panels which are supported by three transverse portal frames, or ‘beams’ as they will be referred to in this paper, spanning the full width of the deck. In total, there are 20 glass panels. The panels on the sides of the ship are planar and are inclined at an angle of 7.8° from vertical. Directly above each side panel is a double curved ‘corner panel’. The top panels, which act as the roof or ceiling of the structure, span between the curved panels and are also double curved, with convex curvature in the transverse plane (y-z plane) as well as slight convex curvature in the longitudinal plane (x-z plane). The minimum radius of curvature in the transverse plane ranges from approximately 870 mm to 1050 mm, and 3810 mm to 8200 mm for the corner and top panels, respectively. The radius of curvature in the longitudinal plane is significantly higher and almost unnoticeable with the naked eye. The side, corner and top panels are indicated in Fig. 2.

It is expected that such glass panels would consist of laminated glass to increase its strength and post fracture rigidity. However, the exact lay-up was not determined in this study. Instead, as is commonly used during the preliminary design phase, the panels are modelled as monolithic glass. To determine the nominal thickness of a glass laminate with similar mechanical behaviour, the enhanced effective thickness (EET) method may be used (Galuppi et al., 2013; Galuppi & Royer-Carfagni, 2012). Typically the EET method is used to model a glass laminate as monolithic glass with an effective thickness. Conversely, the laminate thickness can also be determined if the monolithic glass panels in the model are considered to have the effective thickness of the laminate and if a certain shear stiffness of the interlayer is assumed. For the modelling of the glass behaviour, it is not necessary to specify pre-stressing of the glass. However, it should be mentioned that the optical quality of the glass of yacht windows is of high importance. For this reason, chemically strengthened glass is often used in yacht windows and is preferred to thermally toughened glass due to its superior visual quality. It does not exhibit anisotropies in the distribution of pre-stress often found in thermally toughened glass where it may result in visual distortions such as the appearance of waves on the glass surface (Laurs et al., 2019; Moupagitsoglou, 2020; Verbaas, 2012).

The three transverse beams, as indicated in Fig. 2, were added to the glass structure to act both as stiffening members for the structure and as a means of dividing the glass structure surface into the separate glass panels. These beams add out-of-plane bending resistance to the glass panels which would otherwise be low considering the size of the glass panels. They also offer structural redundancy in a scenario where one glass panel breaks and allow for easier replacement of individual glass panels in the case of fracture.

The proposed connection method between the glass panels and the beams is adhesive bonding. As opposed to mechanical connections, such as bolts and clamps, adhesive connections allow forces to be spread over a larger glass area which lowers stress concentrations. Holes also do not need to be drilled for bolts, where high stresses also tend to occur (Dispersyn & Belis, 2016; Van Lancker et al., 2016). Even though the superstructure of yachts of this size are generally made of aluminium, it was decided to use steel beams due the higher Young’s modulus of steel. This would also result in smaller beam profiles as opposed to aluminium beams. It is expected that stainless steel would be used for this application due to it’s corrosion resistance which would avoid having to coat the steel in paint or an anti-corrosion coating. A hollow rectangular profile with a height of 200 mm, a width of 100 mm and a thickness of 12.5 mm was chosen for the beams. The rectangular shape was chosen as it offers a

surface on to which the glass panels can be bonded and the hollow section allows for any electronic apparatus to be fitted in the structure, such as cables and light fittings.

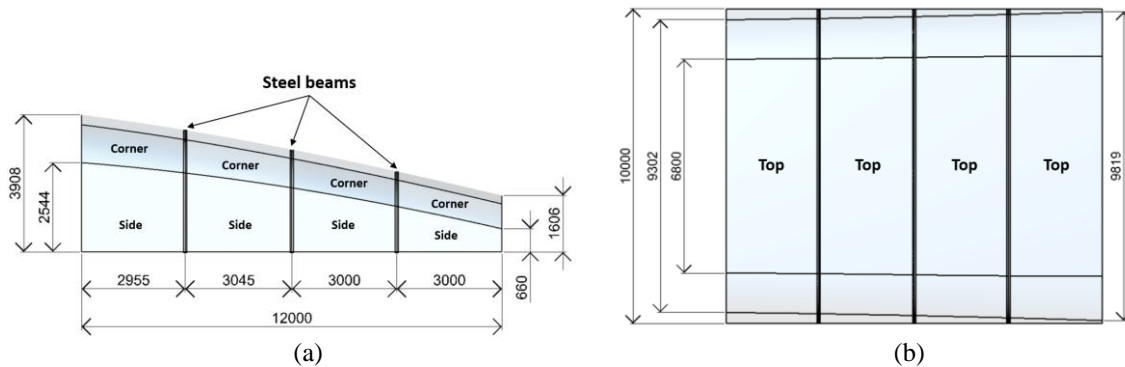


Fig. 2: Main dimensions of glass structure in millimeters. (a) Side (starboard) view. (b) Top view.

The original structure in way of the glass structure is entirely removed from the deck upwards. The shape of the glass panels were modelled such that they follow the curvatures of the original structure, both in the longitudinal and transverse directions. This creates a sense of continuity from aluminium surface to glass surface.

3. Loads and load cases

Yachts are typically exposed to loads which may be labelled as either ‘global’ or ‘local’ loads. Global loads act on the hull of the ship and cause global deformation, while local loads act over smaller areas of the structure and cause local deformation (Wium et al., 2022). In this study, the loads acting on the glass structure were chosen with reference to the technical standards of classification societies. Classification societies are non-governmental organizations which set technical standards for the design and scantling rules of ships. These standards or ‘rules’ pertain to the strength and integrity of the ship structure, the machinery and equipment, but do not guarantee seaworthiness which is ultimately the responsibility of the ship owner and operators. Building a yacht according to classification society rules is generally voluntary. However, this is commonly done to fulfil requirements of the country in which it is registered (flag state) and for insurance purposes. During the design and construction of a ship there is a close cooperation between the designers, the builders and a classification society to ensure the ship conforms to the technical standards. In this study, the rules of three classification societies were considered: Lloyd’s Register’s Rules and Regulations for the Classification of Special Service Craft (LR) (2020), DNV Rules for Classification Yachts (DNV) (2022) and Bureau Veritas NR500 Rules for the Classification and Certification of Yachts (BV) (2022).

A global load analysis was performed according to a guideline of Lloyd’s Register for the assessment of the primary structure of passenger ships using finite element method (Lloyd’s Register, 2019). The longitudinal bending of the hull arising from waves moving in the x-axis of the ship and the weight of the ship was determined. Transverse and torsional bending of the hull was neglected, as this is typically small for monohulls of this length (Lloyd’s Register, 2020). The maximum bending of the ship is simulated, which occurs when the length of a wave is approximately equal to the length of the hull. The ship will then either bend upwards or downwards, depending whether the hull is on top of the crest or within the trough of the wave. According to the guideline of Lloyd’s Register, an additional case is considered to check the strength of the structure with regards to a maximum shear force amidship while transitioning between a crest and a trough. It was found that the deformation of the superstructure in these simulations will not have a significant effect on the structural behaviour of the glass structure, due to the location of the glass structure within the ship. Therefore, in this paper the deformation of the yacht due to global loads is neglected. The remaining local loads which are of significance to the glass structure are hydrodynamic pressures from waves and water splashing onto the structure, wind pressure, snow loads, the self-weight of the structure, and inertial accelerations due to the motion of the ship in waves.

For the calculation and the implementation of the local loads in the FE model, the rules of classification societies were also followed. Classification societies often specify a design pressure for superstructure external plating which accounts for a range of possible loads the structure can be exposed to. This may include, hydrodynamic pressures originating from waves or bodies of water splashing against the ship (green water), snow loads, wind loads, and cargo and passenger weights. The design pressure represents the maximum possible pressure expected during the operation of the ship. The strength of local scantlings are assessed against this design pressure.

Table 1 gives the design pressures for the sides of the superstructure based on the locations of the glass panels. These pressures are for metallic plating and not for glass panels used as integrated structural components, which are not dealt with in classification society rules. Design pressures were calculated according to LR, DNV and BV. For comparison, the design pressure for glass panes in yacht windows are also given in Table 1, calculated according to ISO 11336-1 (2012). However, a design pressure for horizontal glass panes, such as the top panels in the glass structure, is not specified in this standard. The side pressures according to DNV, BV and ISO, is a function of longitudinal and vertical position, and according to LR, only a function of longitudinal position. One longitudinal and vertical coordinate is chosen for the calculation of the pressures acting on the side and corner panels, since the pressures across these panels do not vary significantly. Halfway along the length of the glass structure is used as the longitudinal position and the bottom edges of the side panels for the vertical position. For the top panels, the design pressures for deck loads were used. The top pressures were calculated at halfway along the length of the structure at the top of the structure.

Table 1: External design pressures for superstructure sides.

Panels	Superstructure side plating pressure			Windows pressure
	BV	DNV	LR	ISO
Side & Corner	5.0 kPa	6.3 kPa	6.2 kPa	16.2 kPa
Top	3.0 kPa	6.9 kPa	3.77 kPa	-

Table 1 shows a variation in the design pressures of the classification societies and of ISO. Most noticeable is the larger design pressure specified by ISO, which is a minimum pressure adopted from minimum requirements of the local lateral loads given by the International Association of Classification Societies (IACS) (2023). These requirements are not specific to yachts, but are recommended for a variety of ship types. On the other hand, the rules of BV, DNV and LR are specific to yachts. For this reason and in keeping with the approach of treating the panels as conventional structural components, the pressures according to these three classification societies are preferred. When comparing the pressures between the three societies, the pressures are within a reasonable range of one another, except in the case of the top pressure per DNV in which case the top pressure is higher than the side and corner pressure. Since the top panels are higher than the side and corner panels, it is reasonable to assume that the loads these panels will experience are lower, as they are less likely to be impacted by water. Therefore, the pressures of BV and LR are more suitable. Furthermore, BV makes a distinction between decks which are not directly exposed to sea pressures and not accessible to passengers and crew members, and decks which are. LR does not make this distinction for the calculation of deck pressures. Since, the description of the deck pressure of BV best describes the case of the top panels in the glass structure, it was decided to use the design pressures of BV in this study. Note that during the design of a ship, the choice of which classification society rules to follow may also depend on the requirements of the flag state or the preference of the shipbuilder.

Using the parameters of the 90 m yacht, design inertial accelerations were calculated according to DNV rules. DNV rules were chosen as they are the only rule among those considered which allows the calculation of inertial acceleration in all three dimensions.

Table 2 gives the magnitudes of the accelerations in the three dimensions, with reference to the axes shown in Fig. 3. The accelerations were calculated at the area centroid of the glass panels. Referring to Fig. 3, x- and z-

accelerations are dominant when the ship is sailing with waves moving in the x-direction (head seas), resulting in mainly surging and heaving motions. When waves are moving in the y-direction (beam seas), the ship is mainly rolling and heaving, in which case y- and z-accelerations are dominant.

Table 2: Inertial accelerations in three degrees.

Longitudinal (x)	Transverse (y)	Vertical (z)
9.21 m/s ²	7.42 m/s ²	11.4 m/s ²

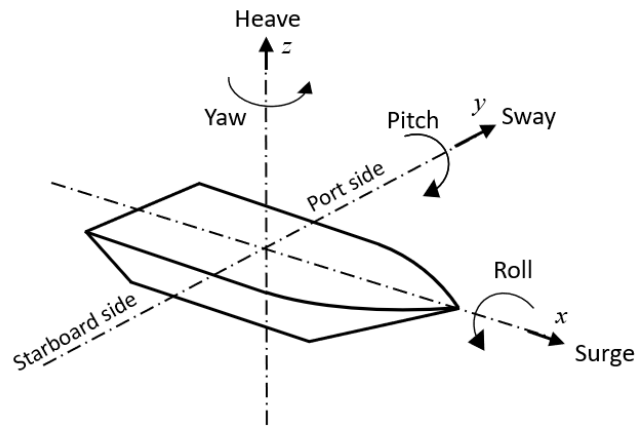


Fig. 3: Ship motions.

Load cases were set up for head seas and beam seas wave conditions. The directions of the inertial accelerations as given in Table 4 correspond with the axes shown in Fig. 3. Table 4 gives the load combinations for each load case and the areas of the glass structure on which the loads are applied.

Table 4: Load cases.

Load case	Wave condition	Design pressure	Inertial accelerations	Gravity
LC1	Head seas	All panels	-	All structure
LC2	Head seas	All panels	x & z	All structure
LC3	Beam seas	Port side & corner panels	y & z	All structure
LC3a	Beam seas	-	y & z	All structure
LC3b	Beam seas	Port side & corner panels	-	All structure

Two load cases are set up for head seas and three for beams seas. LC1 and LC2 represent a case where the entire structure is under hydrostatic pressure, simulating water from a large wave splashing onto the ship. In LC1, the ship is assumed to be static and in LC2, the ship is assumed to be heaving and pitching with the corresponding inertial accelerations.

LC3 represents a case where the ship is in beam seas and inclined towards the port side. Here water is assumed to impact the port side when waves are moving perpendicular to the port side of the hull. The design pressure is applied to the port side and corner panels, as well as the port half of the top panels. The corresponding inertial accelerations are applied to simulate rolling and heaving motion as the ship is returning to its upright position after being inclined towards the port side. In this case, the vertical acceleration is applied in opposite directions on the port and starboard side to exaggerate the rolling motion of the glass structure about the centerline. The vertical acceleration is applied upwards on the port side and downwards on the starboard side with the maximum acceleration at the extremities of the width of the structure. The accelerations change linearly across the width of the structure from positive to negative. LC3a and LC3b were created to compare the respective effects of designs pressure and inertial accelerations.

4. Simple connection FE model

An FE model of the glass structure was created in the commercial FE software Abaqus (version 2020). This FE model will be referred to as the ‘simple connection model’. The monolithic glass panels were modelled with 4-node linear shell elements with reduced integration (S4R elements) and a target size of 50 x 50 mm over the whole panel. The transverse steel beams were modelled with 2-node 1-D beam elements (B31), also with a target length of 50 mm. Fig. 4 shows the FE model of the glass structure.

The glass of the panels is assumed to be soda-lime silica glass and is taken as an isotropic material with linear elastic material behaviour. Table 5 gives the material properties of the steel beams and the glass panels which were used in the FE model.

Table 5: Materials used in FE model.

Material	Young’s modulus	Poisson ratio	Density
Steel	200 GPa	0.3	7800 kg/m ³
Soda-lime silica glass	70 GPa	0.22	2500 kg/m ³

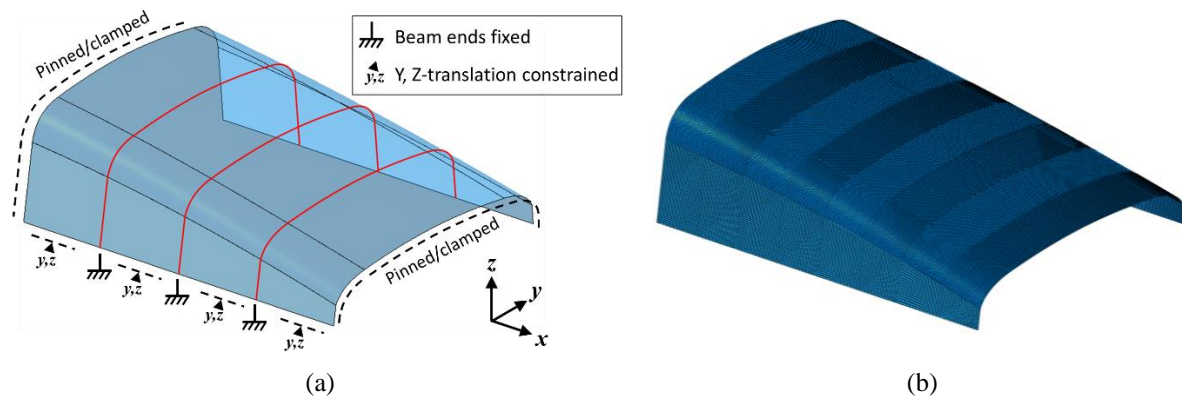


Fig. 4: a) Geometry of the beams and panels in the FE model with boundary conditions. B) FE model mesh.

The connections between the transverse beams and the panels are simplified by either modelling a ‘pinned’ or ‘clamped’ connection between the edges of the panels and the beams. Further details of the connection, such as adhesive bonding or other mechanical components are not modelled. This is done to reduce the computational time of the FE model and to assess how the type of connection (pinned or clamped) influences the behaviour of the model before more detailed modelling methods are implemented. Node-to-node tie constraints are used to connect nodes on the edges of the glass panels to the nodes of the beams. Fig. 5 indicates node-to-node tie constraints between nodes on the panes and a node on the beam. For the pinned connection type, only the translational degrees of freedom are tied while both translational and rotational degrees of freedom are tied for the clamped connection. In general, there is a gap of 2 mm between all glass panels. The gap is solely for the purpose of disconnecting the panels from each other. No contact is recognized between the panels, even if their edges would intersect. In practice, a sealant would need to be applied between such a gap between the panels to create a watertight and weathertight structure. However, in this study the type of sealant is not established and it is assumed the sealant has no load transferring capabilities.

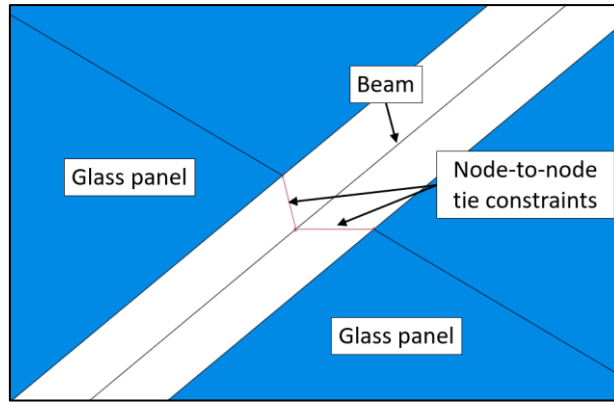


Fig. 5: Node-to-node tie constraints indicated between the node of a 1-D beam element and the nodes of the shell elements of the glass panels.

As shown in Fig.4a, translation of the bottom edges of the glass panels are constrained in the lateral (y) and vertical (z) directions. Vertical movement of the edges are prevented to simulate the panels resting on the deck with the weight of the structure preventing any lift-off. It is also assumed the panels will be bonded at the bottom to an aluminium plate perpendicular to the deck, preventing transverse movement of the edges but allowing longitudinal (x) movement if a very flexible adhesive is used. A pinned or clamped boundary condition is imposed on the glass edges at the forward and aft ends of the structure, coinciding with the connection type active in the beam-panel connections. The ends of the transverse beams are constrained in translation and rotation.

In Abaqus, the design pressures and wind pressure are applied as a ‘pressure’ load type with uniform distribution. Gravity and inertial accelerations are applied as a ‘gravity’ load type.

5. Parametric study

A parametric study was performed using the simple connection model. The use of a pinned or clamped beam-panel connection type is compared to provide insight into how the behaviour of the connections influence the structural behaviour of the glass structure. This information can aid in identifying the requirements of future connection designs. For each connection type, 20 mm, 30 mm and 40 mm glass panel thicknesses were also considered. The different glass panel thicknesses were varied to determine the extent to which the stiffness of the glass panels influences the behaviour of the overall glass structure. Table 6 presents the 6 parametric configurations that were considered. As a preliminary design step, linear static analyses were performed for each load case (non-linear analyses will be considered in future detail studies).

Table 6: FE model parametric configurations.

Configuration	Connection type	Glass panel thickness
1	Pinned	20 mm
2	Pinned	30 mm
3	Pinned	40 mm
4	Clamped	20 mm
5	Clamped	30 mm
6	Clamped	40 mm

5.1. Results

In this section, the results of the parametric study are presented. For each of the load cases listed in Table 4, the deflections of the beams and the panels, the von Mises stresses in the beams, and the maximum principal stresses in the glass panels are given. These results are extracted from the FE model as they are deemed to be sufficient for the evaluation of the structure on a conceptual level before more detailed analyses, e.g. vibration and buckling, are performed using more detailed FE models. Fig. 6 to Fig. 9 gives the maximum value of each of these output variables in the overall structure for a pinned and clamped beam-panel connection and for glass panel thicknesses of 20 mm, 30 mm and 40 mm. The maximum von Mises stresses and maximum deflections of the beams are presented in Fig. 6 and Fig. 7, respectively. Fig. 8 and Fig. 9 gives the maximum principal stresses and maximum deflections of the glass panels, respectively.

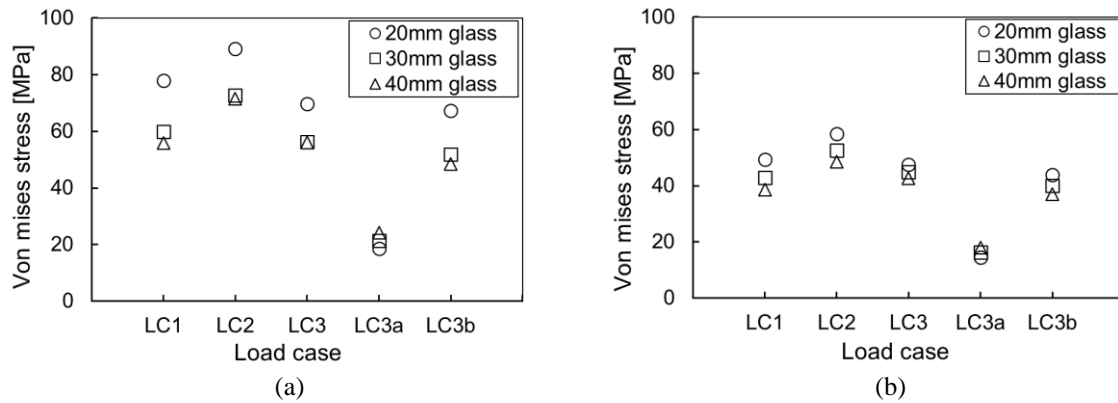


Fig. 6: Maximum von Mises stresses of steel beams.
a) Pinned beam-panel connections. B) Clamped beam-panel connections.

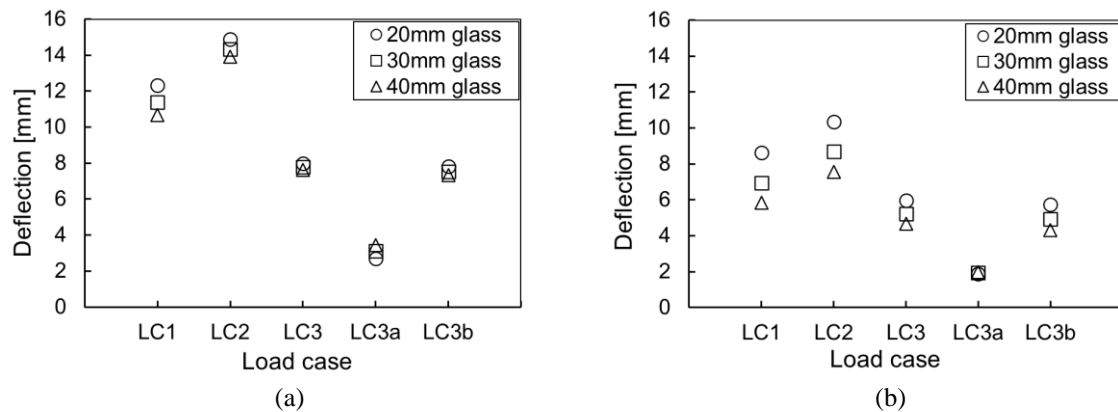


Fig. 7: Maximum deflections of steel beams.
a) Pinned beam-panel connections. B) Clamped beam-panel connections.

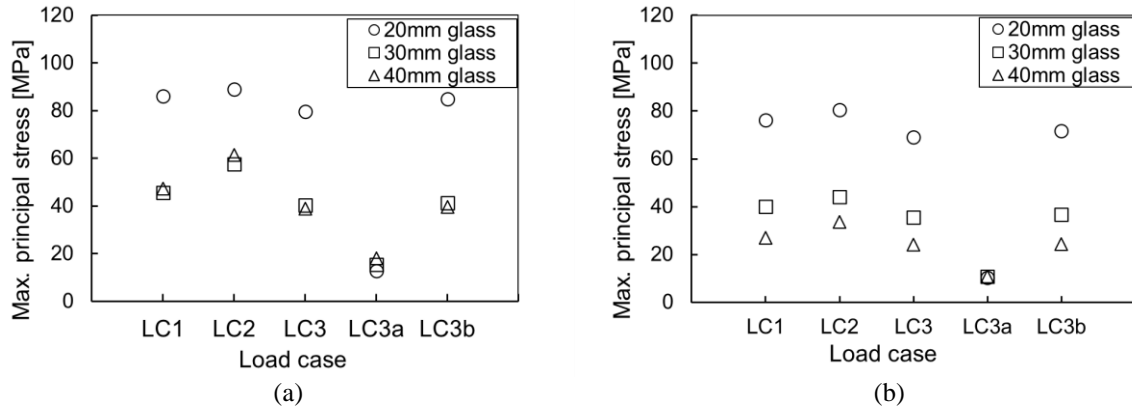


Fig. 8: Maximum principal stress in glass panels.

a) Pinned beam-panel connections. B) Clamped beam-panel connections.

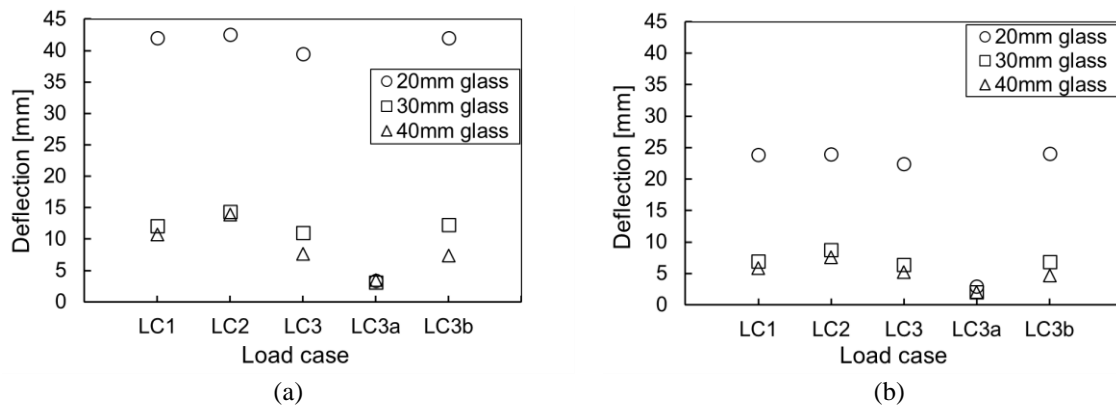


Fig. 9: Maximum deflections of glass panels.

a) Pinned beam-panel connections. B) Clamped beam-panel connections.

5.2. Discussion

The calculation of the permissible stresses for beams in the superstructure of a yacht varies among classification society rules. Nevertheless, the maximum von Mises stresses in the beams for each glass structure configuration and load case is well below a theoretical yield stress of 205 MPa for stainless steel. Fig. 10 indicates the location of the maximum von Mises stress in the beams for each parametric configuration. Load case LC2 resulted in the highest stress for all configurations. The maximum deflections of the beams are also found for LC2 and the point of maximum deflection is at the top of the central beams for all configurations, as shown in Fig. 11. There is currently no criteria for the allowable deflections of such a glass structure in a yacht. However, treating the transverse beams as conventional stiffeners in the superstructure, LR specifies a span to deflection ratio of 600. Assuming the span of one of the transverse beams is between the corner panels, this results in an allowable deflection of approximately 12 mm. Deflections less than 12 mm is achieved for the clamped beam-panel connection for all three panel thicknesses. For glass panes in conventional yacht windows, ISO 11336-1 (2012) specifies an out-of-plane allowable deflection where the deflection of the pane is not allowed to exceed 1/50 of the length of the long side of the window. Applying this criterion to the largest top panel in the glass structure, gives an allowable deflection of 140 mm, which is well above the deflections found in the simple connection model. Note that due to the high deflections of the 20 mm panels, exceeding half the thickness of the panels, membrane action may be present. In this case non-linear geometric analysis can more accurately capture the behaviour of the panels (Moupagitsoglou, 2020).

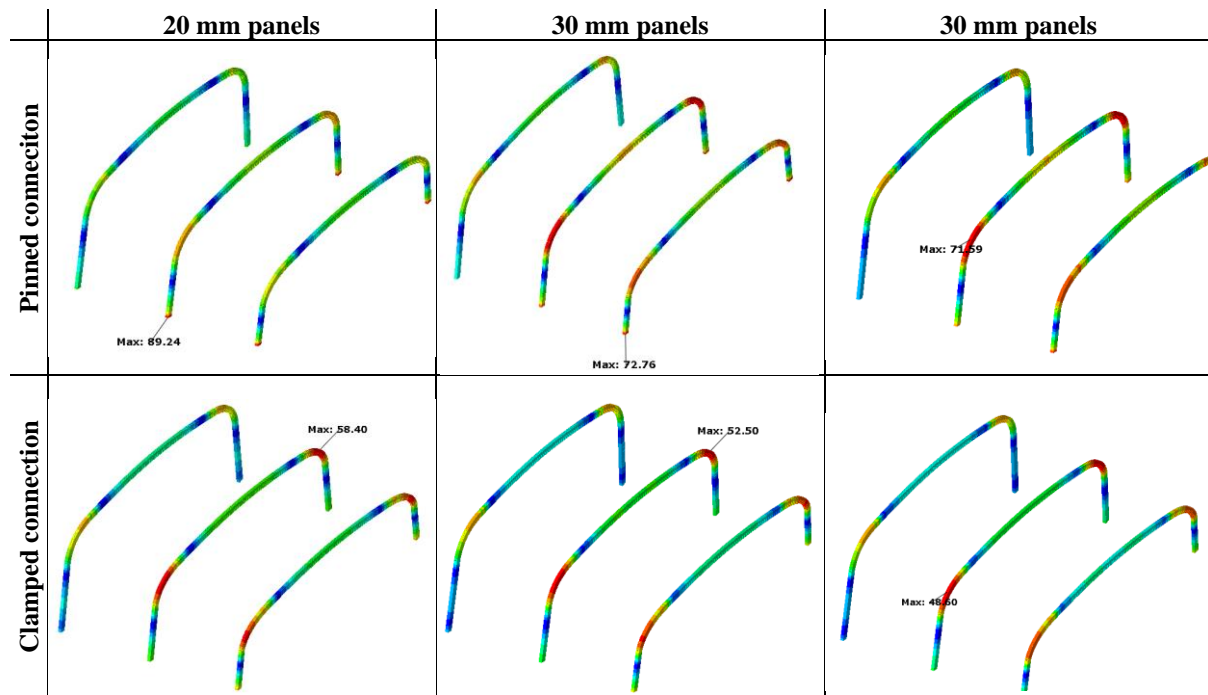


Fig. 10: Isolated view of beams showing location of maximum von Mises stress for each parametric configuration for load case LC2.

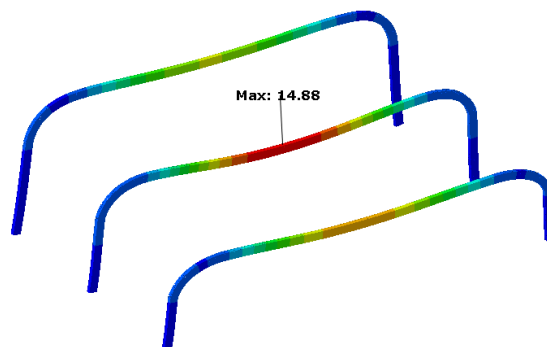


Fig. 11: Isolated view of beams showing the location of maximum deflection of the pinned beam-panel connection with 20 mm thick panels. Deformation is visually scaled by 50.

ISO 11336-1 (2012) also specifies a minimum failure strength which glazing materials of different types of glass and pre-stressing processes should meet. A design strength is then calculated using a design factor. However, as ISO 11336-1 (2012) only considers the glass pane to act as a conventional window, subjected to out-of-plane loading, it would be more relevant to calculate a design strength according to the international technical standard CEN/TS 19100-1 (2021) which provides methods for calculating the strength of structural glass components. According to CEN/TS 19100-1, the design strength of the largest top panel of the structure is approximately 50 MPa. For this strength calculation, the glass panel is assumed to be thermally toughened due to the lack of input factors for chemically strengthened glass. The edges of the as-produced annealed glass are also assumed to be polished. Note also that the calculation assumes a maximum edge length of 6 m and a maximum surface area of 18 m², both of which are exceeded by the top panels of this glass structure. The maximum principal tensile stresses in the glass structure exceeding 50 MPa is found for a monolithic panel thickness of 20 mm, and for a pinned beam-panel connection in load case LC2 for all three panel thicknesses.

In Fig. 6, the von Mises stresses in the beams show a reduction in values for the clamped connection type across all load cases. This can be owed to the clamped connection allowing for a larger contribution of the glass panels to the bending resistance of the beams. When comparing LC1 to LC2 and LC3 to LC3b, it can be seen that the combination of design pressures and inertial accelerations produce higher beam stresses and deflections than design pressures alone. The largest difference in von Mises stresses between LC1 and LC2 is 16 MPa, which is found for a pinned beam-panel connection and a panel thickness of 40 mm. Between LC3 and LC3b, the largest difference in von Mises stresses is 8 MPa, also found for the pinned connection and a panel thickness of 40 mm. Similar trends are seen in the stresses and deflections of the glass panels for LC1 and LC2, as shown in Fig. 8 and Fig. 9. However, for the stresses and deflections of the panels for LC3 and LC3b, the combination of pressures and inertial accelerations results in lower panel stresses and deflections, due to these two load acting in opposite directions to each other in the transverse direction.

The thickness of the panels directly influences the magnitudes of the inertial accelerations, with thicker panels resulting in larger panel mass which increases gravitational and inertial forces. On the other hand, it is clear from the results that thicker panels also decrease the stresses and deflections of both the beams and the panels.

For each of the maximum principal stresses in the glass panels shown in Fig. 8, the stresses are found to be highly concentrated at corners of the panels. As an example, the maximum stress is given for pinned and clamped beam-panel connections with 30 mm thick panels in Fig. 12a and Fig. 12b, respectively. These stress concentrations occur due to the node-to-node tie constraints between nodes on the edges (and corners) of the panels and the nodes on the beams. Refining the mesh in these areas did not reduce the stress concentrations. If adhesive bonding is to be used between the panels and the beams, the node-to-node tie constraints unrealistically restricts relative movement between the panels and the beams, resulting in the corner stress concentrations. To alleviate the stress concentrations and to simulate an adhesive bonding connection, another FE model is created as presented in Section 6.

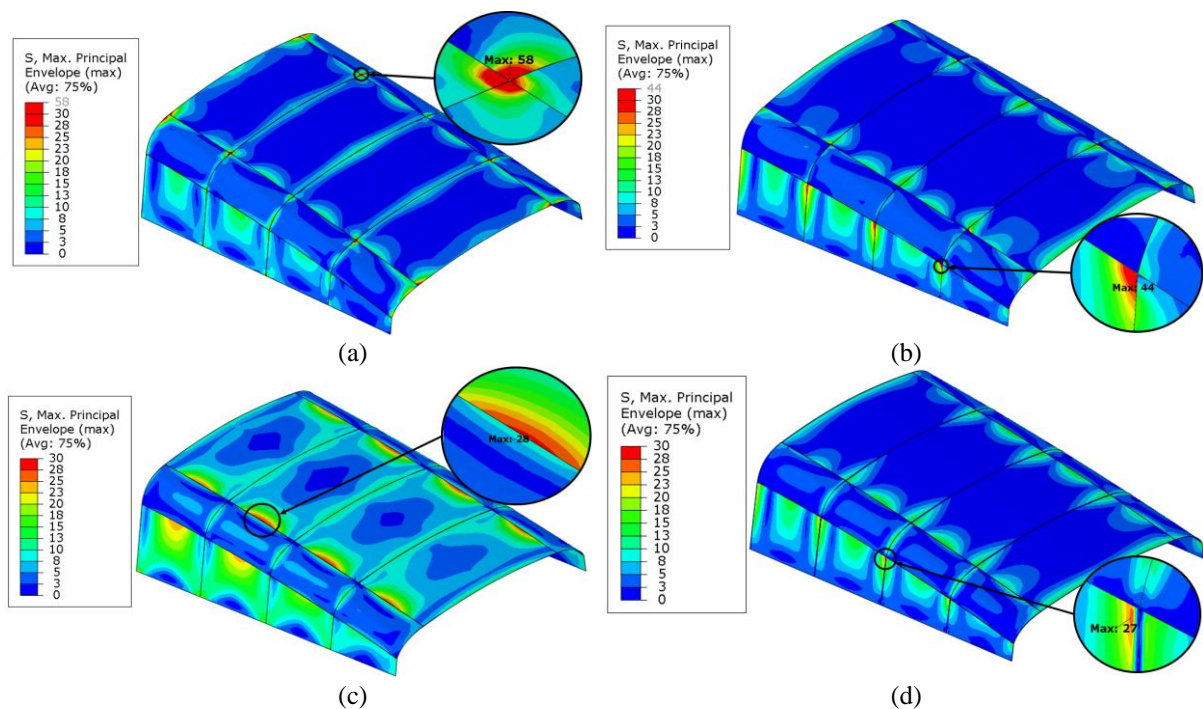


Fig. 12: Maximum principal stresses in glass panels for load case LC2.

- a) Pinned beam-panel connections and 30mm thick panels. b) Clamped beam-panel connections and 30 mm thick panels. c) Cohesive behaviour model with $K_{\text{shear}} = 0.5$ MPa. d) Cohesive behaviour model with $K_{\text{shear}} = 33$ MPa.

As is shown in Fig. 9, for both clamped and pinned connections, deflections of the glass panels are significantly reduced by increasing the monolithic thickness of the panels from 20 mm to 30 mm. However, further increasing the thickness to 40 mm has less of an influence on the deflections. The location of the maximum deflections of the panels also depends on the glass thickness. Fig. 13 depicts the locations of the maximum deflection of the panels for each configuration of the structure, specifying the load case at which the maximum deflection occurs. For 20 mm panels the maximum deflection occurs on the free edge of one of the side panels. The deflections of the free edges will need to be considered when choosing an appropriate sealant based on its strain capabilities.

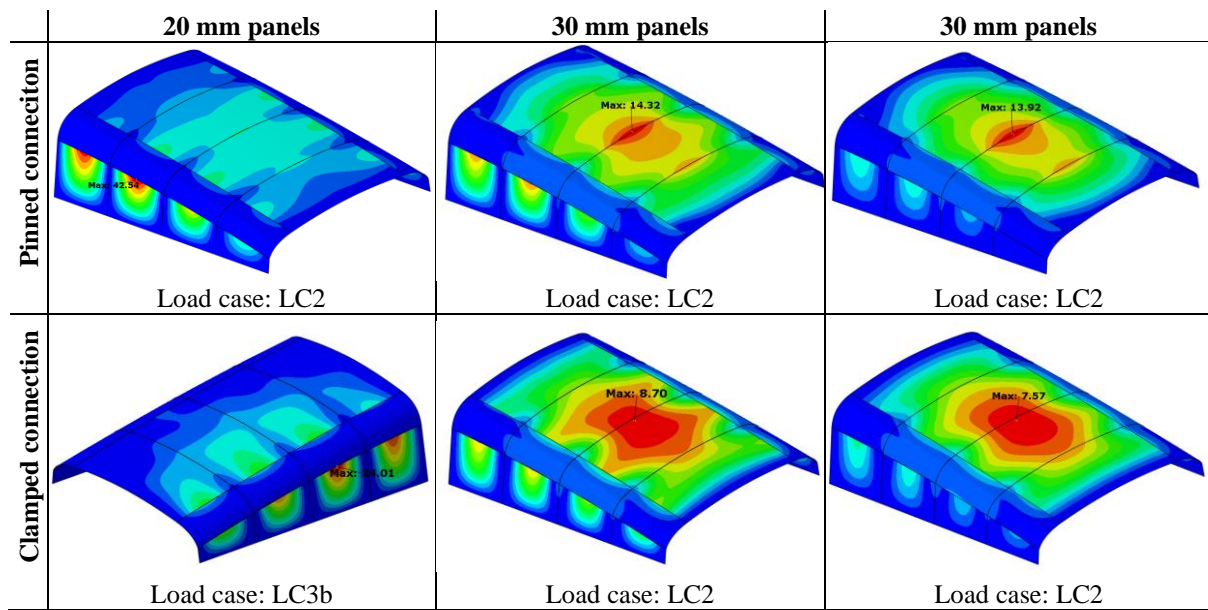


Fig. 13: Maximum deflection of glass structure for each parametric configuration for a corresponding load case.

6. Modelling beam-panel adhesive bonding

A second FE model of the glass structure was created in which the behaviour of an adhesive bond between the glass panels and the transverse beams is approximated. This FE model is termed the ‘cohesive behaviour model’. The purpose of this model is to show how the use of adhesive bonding can be used to alleviate the stress concentrations at the glass corners, as found with the simple connection model, while offering sufficient rigidity between the glass panels and the beams.

6.1. FE model

A surface-to-surface contact function with cohesive behaviour in Abaqus is used to connect the glass panels to the steel beams. This function is chosen for its ability to simulate an adhesive connection without modelling elements for the adhesive material, which would otherwise require a large number of solid elements to accurately capture the material behaviour (Fricke et al., 2014; Katsivalis et al., 2018; Wiegard et al., 2018). Instead, a linear elastic relationship is defined between the two surfaces. This only approximates the behaviour of a real adhesive, which, depending on the type of adhesive, may exhibit viscoelastic or hyperelastic material behaviour (Overend et al., 2011; Van Lancker et al., 2020). The contact function also assumes a perfect bond between the glass and the steel. Any debonding or damage to the adhesive connection is not simulated in this study.

The stiffness between the surfaces can be defined in three dimensions using two parameters for the in-plane stiffness (K_t and K_s) and one parameter for the out-of-plane stiffness (K_n). These stiffness parameters can be

related to the Young's modulus (E_{adh}), shear modulus (G_{adh}) and thickness (t_{adh}) of a linear elastic adhesive using Equation 2 and 3:

$$K_n = \frac{E_{adh}}{t_{adh}} \quad (2)$$

$$K_t, K_s = \frac{G_{adh}}{t_{adh}} \quad (3)$$

In this study, K_t and K_s were assumed to be equal and will be referred to as K_{shear} . The ratio between K_{shear} and K_n is based on the linear elastic relationship $E_{adh} = 2(1+\nu)G_{adh}$, where ν is the Poisson's ratio. The theoretical Poisson's ratio of adhesives can vary greatly, depending on the type of adhesive and its chemical composition, and may range from 0.3 to 0.49 (Alexandru et al., 2019; Overend et al., 2011). For this study, a Poisson's ratio of 0.45 is chosen, which results in an approximate K_{shear} to K_n ratio of 1:3. Seven stiffness parameter pairs were considered, ranging from a K_n of 1.5 MPa/mm and a K_{shear} of 0.5 MPa/mm, to a K_n of 100 MPa/mm and a K_{shear} of 33 MPa/mm. A range of stiffnesses is chosen to show how the stiffness of an adhesive bond influences the behaviour of the overall glass structure. These stiffnesses also represent adhesives with a structural function, exhibiting higher stiffness and strength than conventional flexible adhesives used for ship windows.

As per Equation 2 and 3, the stiffness parameters can be related to the stiffness of a real adhesive product when assuming a bond thickness. These adhesives may be of different types. In practice, each type of adhesive is applied in a certain bond thickness range for optimal performance. For instance, the thickness of flexible polyurethane adhesives, commonly used to bond yacht windows, can range from 10 mm to 25 mm. More stiff and rigid adhesives, such as epoxies and acrylates are applied in thicknesses less than 1 mm for optimal strength. Applying such thin layers (< 1 mm) of adhesive across the length of the beams would pose a challenge due to the possible variability in the geometric tolerances of the structure. Therefore, assuming a thickness of 10 mm will correspond to a shear modulus ranging from 5 MPa to 330 MPa. This range may represent structural polyurethane adhesives on the lower end as well as epoxy and acrylate adhesives with sufficient flexibility at the other end. Silicone adhesives are generally avoided in superyacht shipyards due to fear of contaminating the paint of the vessel.

The monolithic glass panels were modelled using S4R elements and a glass thickness of 30 mm was chosen for the model. To create a surface on to which the panels can be bonded, the hollow rectangular steel beams were also modelled with S4R elements to create the rectangular profile. Fig. 14a shows a cross section of one of the beams with the panels in contact. The surface of the panel which is in contact with the beam has a width of 49 mm. This leaves a 2 mm gap between panels bonded to the beams. As depicted in Fig. 14, a target element size of 10 mm is set at the bonding edge of the panels, which increases to 100 mm at the center of the panels. Element sizes were reduced in the vicinity of the beam-panel interface as part of a mesh convergence study to improve the accuracy of the surface-to-surface contact function, as recommended by the Abaqus Interactions Guide (Abaqus, 2017). An element size of 20 mm was assigned to the elements of the steel beams. The influence of further refinement of the size of the elements of the beams will be determined in future studies.

For the forward end (closest to the bow) and aft end (closest to the stern) of the glass structure, a continuous 50 mm wide and 20 mm thick steel plate is used to represent an interface with the yacht structure on to which the glass panels could be bonded using the surface-to-surface contact function. The steel plate was assigned an element size of 12 mm and is shown in Fig. 14b. The same cohesive behaviour properties, as used for the beam-panel interface, is used. The aft edge of the aft-end bonding plate and the forward edge of the forward-end bonding plate is fixed in translation and rotation.

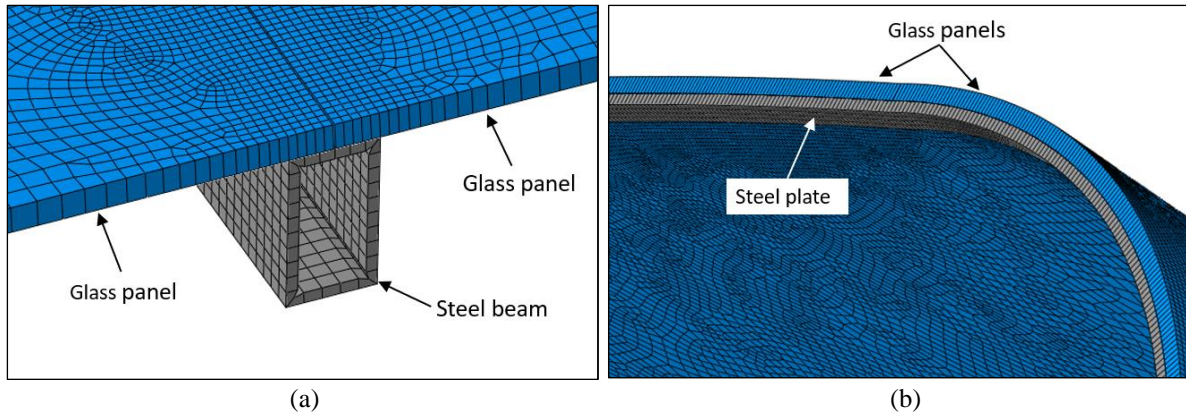


Fig. 14: Shell elements with shell thicknesses activated only for visual purposes.

a) Cross section of FE model at beam-panel interface. b) Steel plate at forward and aft end of glass structure.

6.2. Results and discussion

In the context of a preliminary design phase, linear static analyses were again performed with the cohesive behaviour model for load case LC2. LC2 is chosen as it was found in the parametric study with the simple connection model to result in the highest stresses and deflections. Thereby, the most severe load case could be assessed.

Fig. 15a shows that the maximum of the maximum principal stresses found in the model for each K_{shear} value is significantly lower than those found for the simple connection model with 30 mm thick panels, across both connection types. This can be attributed to the use of the surface-to-surface contact behaviour function allowing relative movement between the panels and the beams, as opposed to the node-to-node tie constraints. The location of the maximum stresses also differs for certain values of K_{shear} . This is the reason why there is a change in the trend of the values of the maximum stresses between a K_{shear} value of 1 MPa/mm and a K_{shear} value of 5 MPa/mm. For a K_{shear} of 0.5 and 1 MPa/mm, the maximum stresses are located at the free edges of the top panels, as shown in Fig. 12c. For all other values of K_{shear} , the highest stresses occur near the edges of the side panels close to the beams, as shown in Fig. 12d. Therefore, more flexible adhesive bonds allow larger rotation of the panel around the beams which increases the bending of a panel and produces larger panel deflection, as indicated in Fig. 15b.

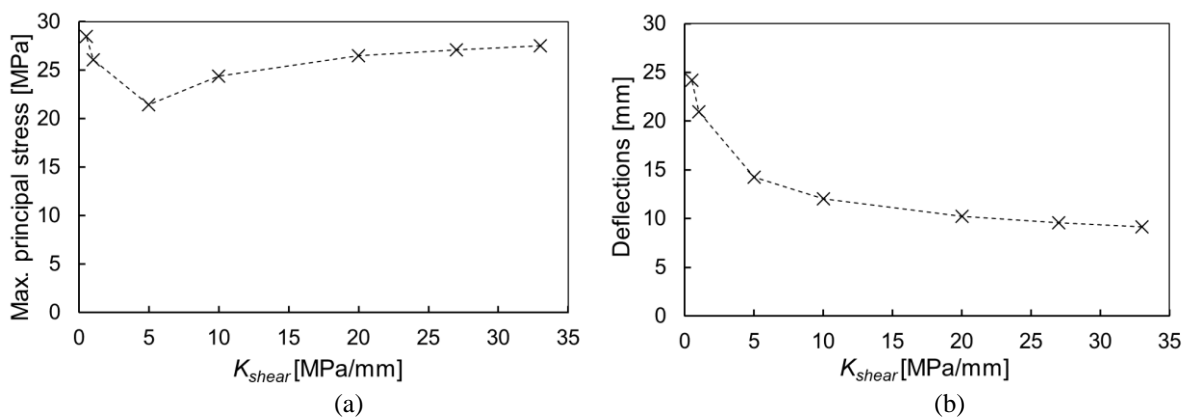


Fig. 15: Cohesive behaviour model a) Panel maximum principal stresses. b) Panel deflections.

Fig. 16 shows that the maximum stresses and deflections of the beams in the model decrease as the stiffness of the cohesive contact increases. This can be compared to the behaviour of the beams in the simple connection model where a pinned and clamped connection is used. Here, a stiffer cohesive contact nears the behaviour of a

clamped connection while a less stiff bond nears the behaviour of a pinned connection. As the glass panels add more stiffness to the structure with a stiffer adhesive, the sizes of the beams could be reduced to increase the transparency of the structure. Fig. 17 shows the location of the maximum deflection and von Mises stress in the steel beams, which is similar for all seven values of K_{shear} .

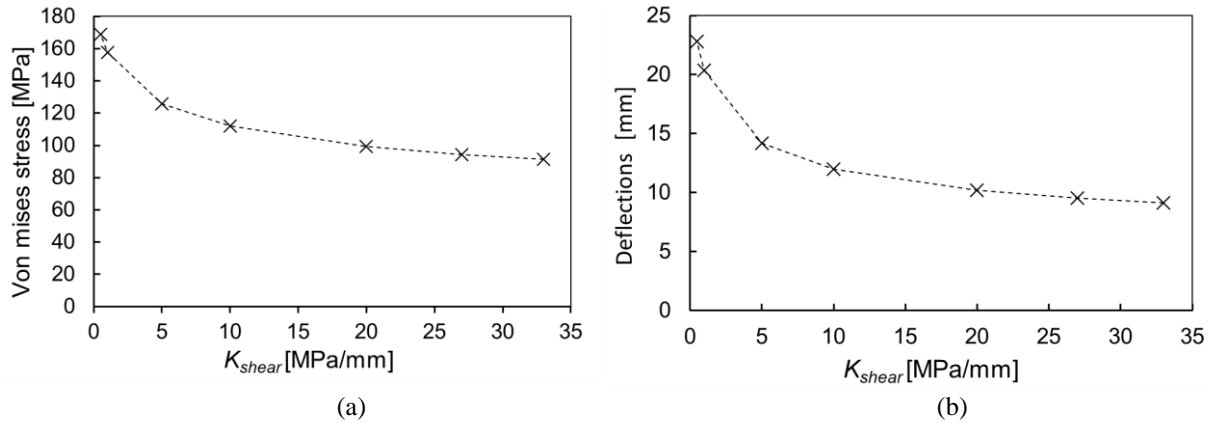


Fig. 16: Cohesive behaviour model a) Maximum beam von Mises stresses. B) Maximum beam deflections.

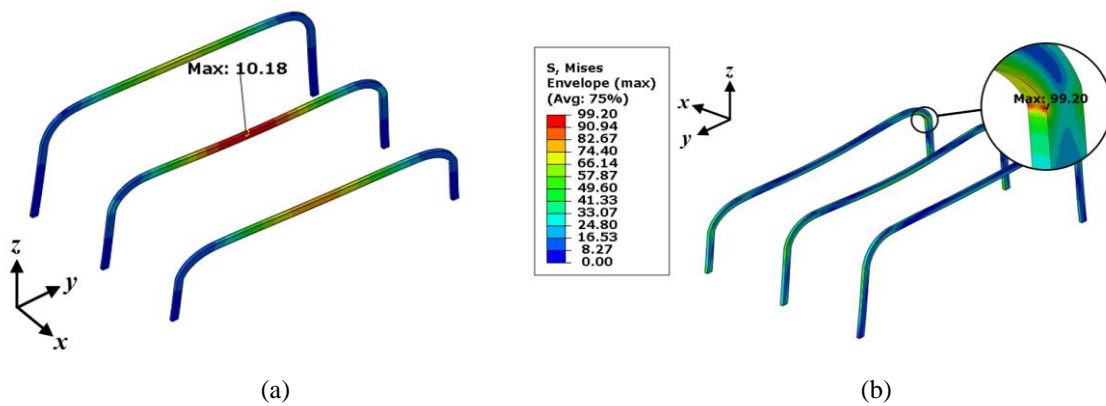


Fig. 17: Isolated view of steel beams of cohesive behaviour FE model for $K_{shear} = 20$ MPa/mm. Deformation is visually scaled by 50. A) Maximum deflection. B) Maximum von Mises stress.

Fig. 18 is shown to indicate how the stresses and strains within an adhesive also have to be considered along with the behaviour of the beams and panels. Even though the stiffness of a selected adhesive may result in favourable stresses and deflections of the beams and panels, the stresses in the adhesive bond may exceed the strength of the adhesive, as well as the maximum elongation of the adhesive. As shown in Fig. 18, higher bond stiffnesses result in higher shear stresses in the adhesive bond, which in turn results in lower adhesive strains. Fig. 19 shows the location of the maximum shear strain in the adhesive bond which coincides with the maximum elongation. Both maximums are found to be at the corner of a top panel.

In the case of more flexible adhesives, e.g. polyurethanes, the elongation of the adhesive poses less of a risk to the failure of the bond and it is more likely that the shear strength of the adhesive is the critical factor. The inverse is generally true for stiffer adhesives such as epoxy and acrylates, where high strength is achieved at the cost of flexibility. The very thin application layers, recommended by manufacturers, for epoxies and acrylates, also poses a problem to both the geometric tolerances of the structure as well as the shear strain capability of the bond. Ideally, the thickness of the adhesive should be increased to lower the shear strains. Although, this might in turn reduce the shear strength of the adhesive. It is recommended that further research be conducted to determine the strength and strain capabilities of stiff adhesives (not limited to epoxies and acrylates) applied in thick layers

(> 10 mm) for applications as presented in this paper. This would allow for the specification of a range of suitable values of K_{shear} which can be recommended to designers.

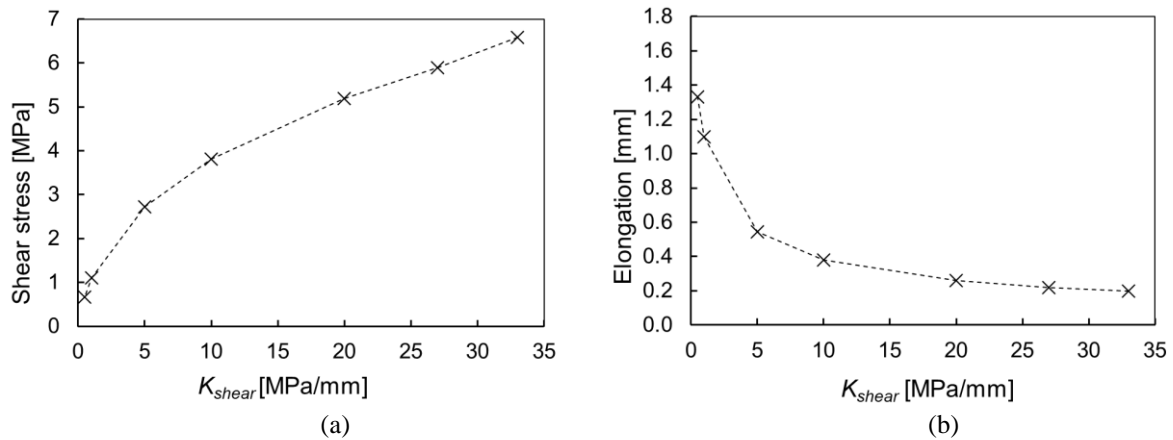


Fig. 18: Cohesive behaviour model a) Maximum bond shear stress. b) Maximum bond in-plane elongation.

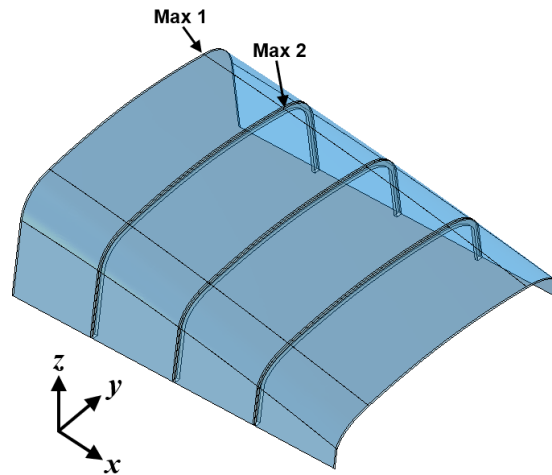


Fig. 19: Location of maximum shear stress and elongation of adhesive bond. Max 1: maximum for $K_{shear} = 0.5, 1, 5, 10, 20$ MPa/mm Max 2: maximum for $K_{shear} = 27, 33$ MPa/mm.

The results of this preliminary study show the instantaneous behaviour of the glass structure under static loading for the chosen cohesive behaviour stiffnesses. In practice, the stiffness of an adhesive may be affected by temperature, load rate, fatigue and long-term exposure to certain environmental factors. Adhesives are prone to degrade after long-term exposure to high temperatures and humidities, UV-radiation and salt concentration (Van Lancker et al., 2016). This could change the initial mechanical properties of an adhesive and should be considered during the design of the adhesive bond and the selection of an adhesive product. Although not evaluated in this study, it should be mentioned that thermal loads can also induce stresses and strains within the adhesive, due to the difference in the coefficients of thermal expansion of the glass and steel.

7. Conclusions

In this study, a parametric study was performed on an FE model of a load bearing glass structure consisting of large glass panels and steel beams in the superstructure of a superyacht. The glass panels in the structure are considered to be an integral part of the superstructure, as opposed to the glass in conventional yacht windows. The results of the parametric study show the following:

- The clamped connection type resulted in a stiffer structure than the pinned connections with lower deflections and reduced beam von Mises stresses.
- Thicker glass panels result in lower maximum principal stresses in the glass. However, increased thicknesses will again increase inertial forces and self-weight due to larger mass.
- For all glass structural configurations, the maximum principal stresses are found to be concentrated at the corners of the glass panels. This is attributed to the use of node-to-node tie constraints between beams and panels.

A second FE model was created to show how the use of adhesive bonding between the beams and the panels can be used to reduce the stress concentrations in the panels. It is shown that the behaviour of the structure is reliant on the stiffness of the adhesive bond between the beams and the panels. Increased bond stiffnesses reduces the deflections of the structure as well as the stresses within the beams, but may increase the stresses in the glass panels. However, when assessing the behaviour of the structure the stresses and strains within the adhesive bond should also be taken into account. Even though the stiffness of an adhesive may result in favourable beam and panel behaviour, stresses and strain in the adhesive may exceed the strength of this adhesive.

Another study is currently underway to determine which adhesive types and adhesive products are most suitable for such an application. Here further research is required into the structural capabilities of suitable adhesives in the marine environment.

Acknowledgements

The assistance of MULTI.engineering and Oceanco by providing information on yacht structures is highly appreciated.

Declarations

Funding:

This research was funded by MULTI.engineering and Flanders Innovation and Entrepreneurship (Agentschap Innoveren en Ondernemen) under Baekeland Mandate HBC.2021.0194.

Conflict of interest:

The authors declare that there is no conflict of interest.

References

Abaqus. (2017). *Abaqus Interactions Guide*. Dassault Systèmes. https://help.3ds.com/2020/english/dssimulia_established/SIMACAEITNRefMap/simaitn-c-contactpairform.htm?contextscope=all

Alexandru, V., Kolany, G., Freytag, B., Schneider, J., Englhardt, O., Silvestru, V. A., Kolany, G., Freytag, B.,

- Schneider, J., & Enghardt, O. (2019). Adhesively bonded glass-metal façade elements with composite structural behaviour under in-plane and out-of-plane loading. *Engineering Structures*, 200(September), 109692. <https://doi.org/10.1016/j.engstruct.2019.109692>
- Boote, D., & Vergassola, G. (2016). Local and global analysis of large motoryacht superstructure. *Proceedings of the 24th International HISWA Symposium on Yacht Design and Yacht Construction*.
- Bureau Veritas. (2022). *NR500 Rules for the Classification and Certification of Yachts* (Issue November).
- Dispersyn, J., & Belis, J. (2016). Numerical research on stiff adhesive point-fixings between glass and metal under uniaxial load. *Glass Structures and Engineering*, 1(1), 115–130. <https://doi.org/10.1007/s40940-016-0009-2>
- DNV. (2022). *Rules for Classification Yachts - Part 3 Hull - Chapter 3 Hull design loads* (Issue July).
- European Committee for Standardization. (2021). *CEN/TS 19100-1:2021 - Design of glass structures - Part 1: Basis of design and materials*.
- Fricke, W., Gerlach, B., & Guiard, M. (2014). Experimental and numerical investigation on the load carrying behavior of large ship windows. *Proceedings of the 33rd International Conference on Offshore Mechanics and Arctic Engineering - OMAE14, 4A*. <https://doi.org/10.1115/OMAE2014-23803>
- Galuppi, L., Manara, G., & Royer Carfagni, G. (2013). Practical expressions for the design of laminated glass. *Composites Part B: Engineering*, 45(1), 1677–1688. <https://doi.org/10.1016/j.compositesb.2012.09.073>
- Galuppi, L., & Royer-Carfagni, G. (2012). The effective thickness of laminated glass plates. *Journal of Mechanics of Materials and Structures*, 7(4), 375–400. <https://doi.org/10.2140/jomms.2012.7.375>
- Gizzi, V., & Bennison, S. J. (2009). New Marine Glazing Developments. *Glass Performance Days 2009*, 149–151. <http://www.glassfiles.com/library/article.php?id=1392>
- International Association of Classification Societies (IACS). (2023). *Requirements concerning STRENGTH OF SHIPS*. <https://iacs.org.uk/publications/unified-requirements/ur-s/>
- International Organisation for Standardization. (2012). *ISO 11336-1: Large yachts - Strength, weathertightness and watertightness of glazed openings - Part 1*.
- International Organisation for Standardization. (2019). *ISO 11336-3: Large yachts - Strength, weathertightness and watertightness of glazed openings - Part 3*.
- International Organisation for Standardization. (2020). *ISO 11336-2: Large yachts - Strength, weathertightness and watertightness of glazed openings - Part 2*.
- Jansen, K. M. (2014). Glass As a Load Bearing Material in Yacht Structures. *Proceedings of the 23rd International HISWA Symposium on Yacht Design and Yacht Construction*.
- Katsivalis, I., Thomsen, O. T., Feih, S., & Achintha, M. (2018). Strength evaluation and failure prediction of bolted and adhesive glass/steel joints. *Glass Structures and Engineering*, 3(2), 183–196. <https://doi.org/10.1007/s40940-018-0070-0>

- Laurs, M., Schaaf, B., Di Biase, P., & Feldmann, M. (2019). Determination of Prestress Profiles in Chemically Toughened Glass by Means of Photoelasticity. *Proceedings of Glass Performance Days 2019 Conference*, 145–149.
- Lloyd's Register. (2019). *Structural Design Assessment - Primary Structure of Passenger Ships* (Issue August). <http://www.lr.org>
- Lloyd's Register. (2020). *Rules and Regulations for the Classification of Special Service Craft* (Issue July). <http://www.lr.org>
- Moupagitsoglou, K. (2020). Structural Glass in Superyacht Applications: Overcoming Challenges, Design Standards and Analysis Methods. *Proceedings of Challenging Glass 7 Conference on Architectural and Structural Applications of Glass*.
- Overend, M., Jin, Q., & Watson, J. (2011). The selection and performance of adhesives for a steel-glass connection. *International Journal of Adhesion and Adhesives*, 31(7), 587–597. <https://doi.org/10.1016/j.ijadhadh.2011.06.001>
- Van Lancker, B., De Corte, W., Belis, J., Lancker, B. Van, Corte, W. De, & Belis, J. (2020). Calibration of hyperelastic material models for structural silicone and hybrid polymer adhesives for the application of bonded glass. *Construction and Building Materials*, 254, 119204. <https://doi.org/10.1016/j.conbuildmat.2020.119204>
- Van Lancker, B., Dispersyn, J., De Corte, W., Belis, J., Lancker, B. Van, Dispersyn, J., Corte, W. De, & Belis, J. (2016). Durability of adhesive glass-metal connections for structural applications. *Engineering Structures*, 126, 237–251. <https://doi.org/10.1016/j.engstruct.2016.07.024>
- Verbaas, F. (2012). Use of Glass and the Regulations. *Proceedings of the 22nd International HISWA Symposium on Yacht Design and Yacht Construction*.
- Wiegard, B., Ehlers, S., Klapp, O., & Schneider, B. (2018). Bonded window panes in strength analysis of ship structures. *Ship Technology Research*, 65(2), 102–121. <https://doi.org/10.1080/09377255.2018.1459066>
- Wium, D., Lataire, E., & Belis, J. (2022). Considerations for the Integration of Glass in Superyacht Structures. *Proceedings of Challenging Glass 8 Conference on Architectural and Structural Applications of Glass*. <https://doi.org/10.47982/cgc.8.442>